

## ELASTIC CONSTANTS OF DIAMOND LIKE CARBON FILMS BY SURFACE BRILLOUIN SCATTERING

A.C. FERRARI<sup>a</sup>, J. ROBERTSON<sup>a</sup>, R. PASTORELLI<sup>b</sup>, M.G. BEGHI<sup>b</sup>, C.E. BOTTANI<sup>b</sup>

<sup>a</sup>Engineering Department, Cambridge University, Cambridge CB2 1PZ, UK

<sup>b</sup>INFM- Dip. di Ingegneria Nucleare, Politecnico di Milano, I-20133 Milano, ITALY

### ABSTRACT

The elastic constants of thin Diamond-Like Carbon (DLC) films supply important information, but their measurement is difficult. Standard nanoindentation does not directly measure the elastic constants and has strong limitations particularly in the case of hard thin films on softer substrates, such as tetrahedral amorphous carbon on Si. Surface acoustic waves provide a better mean to investigate elastic properties. Surface Brillouin scattering (SBS) intrinsically probes acoustic waves of the wavelength which is appropriate to test the properties of films in the tens to hundreds of nanometers thickness range. SBS can be used to derive all the isotropic elastic constants of hard-on-soft and soft-on-hard amorphous carbon films of different kinds, with thickness down to less than 10 nm. The results help to resolve the previous uncertainties in mechanical data. The Young's modulus of tetrahedral amorphous carbon (ta-C) turns out to be lower than that of diamond, while the moduli of hydrogenated ta-C (ta-C:H) are considerably lower than those of ta-C because of the weakening effect of C-H bonding.

### INTRODUCTION

The elastic constants of DLC film are important, since they determine the behaviour of the film and because they offer information on film structure, being strongly dependent on the relative abundance of different kinds of carbon-carbon bonds. A network of  $sp^3$  carbon sites, with the high angular rigidity of such bonds, is expected to correspond to high values of the elastic moduli, like Young's modulus or hydrostatic modulus, and to relatively low values of Poisson's ratio (the material is particularly reluctant to undergo shape changes). A network of  $sp^2$  carbon sites has bonds with much lower angular rigidity, and is expected to have substantially lower elastic moduli, like those of disordered graphite, and higher values of Poisson's ratio (the material is prone to undergo shape changes). The presence of hydrogen sites eases shape changes and therefore increases Poisson's ratio. Scaling laws have been proposed, which correlate the elastic moduli with the mean atomic coordination number [1].

A reliable measurement of elastic moduli, such as elements  $C_{ij}$  of the elastic tensor, Young's modulus  $E$ , shear modulus  $G$  and bulk modulus  $B$ , and of Poisson's ratio  $\nu$  is not easy in the case of thin films. These quantities are not independent: the relations among them are well known and not trivial, and in the isotropic case they are all determined by only two independent parameters. However a technique like nano-indentation directly supplies the hardness and only a combination of  $E$  and  $\nu$  [2-6]. Furthermore for film thickness below  $\sim 1 \mu\text{m}$  the requisite of indentation depth significantly smaller than film thickness is difficultly met, and, especially for hard films on softer substrates, the behaviour of the substrate affects the result. Probably due to these difficulties, measurements of Young's modulus of tetrahedral amorphous carbon (ta-C) films by nano-indentation are widely scattered, from 400 GPa to 1100 GPa [3, 4, 6].

Surface acoustic waves (SAWs), i.e. long wavelength acoustic phonons, provide in principle a better way to investigate the elastic constants, because they involve much smaller local strains and because their velocities can be accurately computed as functions of the elastic

properties. The propagation velocity of SAWs can be measured by laser spectroscopic methods, exploiting either thermally activated SAWs (surface Brillouin scattering, SBS) [7] or SAWs excited by laser irradiation (laser induced SAW, LISAW) [8], or by quantitative acoustic microscopy. The spatial resolution of these methods is determined by the wavelength of the phonons being probed. LISAW and acoustic microscopy typically work at a frequency of a fraction of GHz, corresponding, for typical elastic properties, to a wavelength of several micrometers. In SBS a wavelength of the same order of laser wavelength (half a micrometer) is selected by the scattering geometry, and typically corresponds to a frequency of several GHz, up to tens of GHz. SBS therefore has an intrinsically better resolution, and is more sensitive to thin film properties. Its drawback is the longer measurement time. In this work the elastic constants of DLC thin films, both ta-C and hydrogenated ta-C films (ta-C:H), are determined by SBS.

## EXPERIMENT

Four films are considered. A homogeneous ta-C film deposited using an S-bend filtered cathodic vacuum arc (FCVA) [9] on Si(100) wafer at room temperature at a mean ion energy of 100 eV and at a deposition rate of about 0.7 nm/s; a layered ta-C thin film deposited with a single bend FCVA system, always on Si(100) wafer; two ta-C:H films of different thickness deposited on Si(100) wafers from acetylene using an electron cyclotron wave resonance plasma source [10]. All the films were preliminary characterised with electron energy loss spectroscopy (EELS), X-ray reflectivity (XRR) [11], ellipsometry and profilometry to obtain  $sp^3$  content, density and thickness. The samples' properties are reported in Table 1. The films are assumed to be elastically isotropic, being amorphous.

SAW velocities of all the samples were measured by SBS, i.e. the inelastic scattering of light by thermally excited SAW via dynamical modulation of the dielectric function of the medium (elasto-optic effect) and/or dynamic corrugation of the surface (surface ripple). An SBS measurement consists in illuminating the specimen by laser light and analysing the spectrum of the scattered light, dominated by the elastically reflected light at frequency  $\Omega$ , but containing the doublet at frequencies  $\Omega \pm \omega$ , shifted by the SAW frequency  $\omega$ . The SAW wavevector  $q_{\parallel}$  is selected by the scattering geometry and the SAW velocity  $v = \omega/q_{\parallel}$  is directly obtained.

SBS spectra for SAW propagation along the [100] direction on the (001) face of the Si substrate were recorded at room temperature in backscattering configuration, with incidence angle  $\theta$  from 30° to 70° (see Fig.1). The incident light is p-polarised; the scattered light is collected without polarisation analysis, and analysed by a tandem 3+3 pass high contrast interferometer of the Sandercock type with a finesse of about 100. The light source was an Argon ion laser operating at  $\lambda = 514.5$  nm. The incident power on the specimen was around 130 mW, focused into a spot of the order of  $10^3 \mu\text{m}^2$ ; structural stability under irradiation was previously ascertained.

Table 1: Samples' properties

Specimen		$sp^3$ content	plasmon energy (eV)	Density ( $\text{g}/\text{cm}^3$ )	Thickness (nm)	Internal stress (GPa)	hydrogen content
ta-C	Homog.	88%	31.8	3.26	76	10	
ta-C (layered)	Ext. lay. int. lay.			2.70 3.24	7 63.5		
ta-C:H		70%	28.4	2.35	70	6	30%
ta-C:H			28.4	2.35	43		

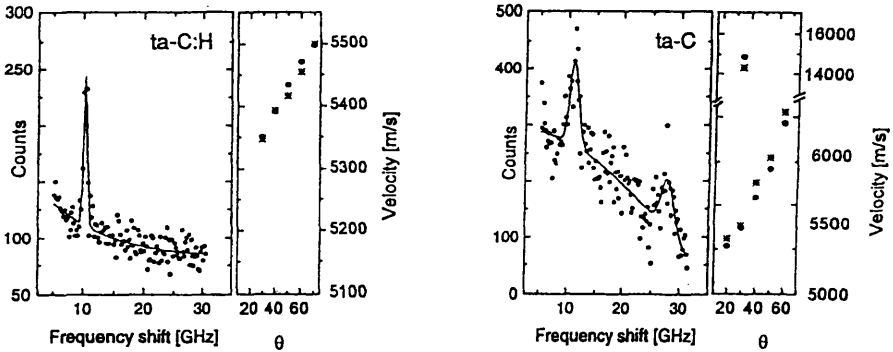


Figure 1. Brillouin spectra at 30° incidence, and measured(\*) and computed(●) dispersion relations of ta-C:H, 70 nm thickness, and layered ta-C specimens. In ta-C:H only the modified Rayleigh wave is visible, while in ta-C the high frequency pseudo-surface wave is also detected.

## RESULTS

The SAW velocities depend on the elastic constants and mass density of both the film and the substrate, on film thickness and on the wavevector  $q_{\parallel}$ . They can be computed [7], allowing the solution of the inverse problem, i.e. the derivation of the elastic constants from measured SAW velocities. The elastic constants and mass density of the anisotropic Si substrate are known ( $C_{11}=166$  GPa,  $C_{12}=63.9$  GPa,  $C_{44}=79.6$  GPa,  $\rho=2.33$  g/cm<sup>3</sup>), as well as the SAW propagation direction and the film thickness and density, supplied by XRR and EELS. Thus the acoustic velocities remain functions of the unknown elastic constants of the film.

An isotropic film has elastic properties fully defined by only two independent quantities, which can be taken among the two elements  $C_{11}$  and  $C_{44}$  of the elastic tensor, the  $E$ ,  $G$  and  $B$  moduli and Poisson's ratio  $\nu$  (for isotropic films  $G=C_{44}$ ). The relations amongst them are well known. The  $(E,G)$  pair turns out to be appropriate for the solution of the inverse problem. The velocities  $v_e^i(E,G)$  are computed at each  $q_{\parallel}^i$  (i.e. at each incidence angle) in a rectangular mesh of values of  $E$  and  $G$ , encompassing a physically significant interval. The couple  $(E,G)_{\text{film}}$  is obtained by a least squares fit of the computed velocities  $v_e$  to the experimental ones  $v_e^i$ :

$$R = \sum \left( \frac{v_e^i(E,G) - v_e^i}{\sigma_e^i} \right)^2 = \min ,$$

where  $\sigma_e^i$  are the variances of the corresponding  $v_e^i$  due to the statistical measurement errors. The  $(E,G)$  couple which minimises  $R$  is the most probable solution of the inverse problem, and the regions corresponding to any fixed confidence level are also obtained.

It must be remembered that the elastic properties of the film, represented by e.g. a point in the  $(E,G)$  plane, must satisfy thermodynamical stability requirements. This means that the  $(E,G)$  plane, like the  $(E,\nu)$  or  $(B,G)$  or similar planes, includes regions which are not physically meaningful. The  $(E,G)$  couple is appropriate for the fitting procedure of the modified Rayleigh wave velocity because this velocity is particularly sensitive to these moduli, and relatively insensitive to the bulk modulus  $B$ . In the  $(E,G)$  plane the  $\nu=\text{const}$  lines are straight lines, and the  $\nu=0.5$  line marks the limit for thermodynamic stability. When approaching or crossing this limit,

the computed SAW velocities remain finite and continuous, but  $B$  diverges. This means that, if  $\nu$  is high and the confidence region falls therefore close to the stability limit, even a small region in the (E,G) plane, i.e. a good determination of both  $E$  and  $G$ , still corresponds to a wide interval of  $B$ , which remains poorly determined.

Generally, the surface projected spectrum of long-wavelength acoustic phonons of given surface wavevector for a homogeneous semi-infinite medium includes a discrete (low-frequency) set and a continuous (high frequency) set. Waves belonging to the discrete spectrum are true surface waves (surface bounded modes), like the Rayleigh wave. In the continuous part, peaks corresponding to wave-packets of bulk waves with a partial surface localization (pseudo-surface waves) can exist. Among the pseudo surface waves the sole relevant excitation of a isotropic surface is the High Frequency Pseudo Surface Wave (HFPSW), also called Longitudinal Resonance (LR) [12], because it propagates parallel to the surface with the velocity of longitudinal bulk phonons and is polarised along its propagation direction. The visibility of LR in a SBS experiment depends on the strength of the elasto-optic coupling, since it does not produce a surface ripple.

A supported film modifies the Rayleigh wave into a Modified Rayleigh Wave (MRW), and the LR into a Modified Longitudinal Resonance (MLR), which becomes a Longitudinal Guided Mode (LGM) if the film is acoustically slower than the substrate and therefore confines the wave. The MLR velocity, differently from the MRW, is strongly sensitive to the modulus  $B$ . The MLR was not detectable in the ta-C:H samples, but it was measured, for at least one incidence angle, in the ta-C samples, supplying additional information that significantly reduces the uncertainty about the  $B$  value and Poisson's ratio  $\nu$ . Further uncertainty reduction comes from physical plausibility. If part of the confidence region in the (E,G) plane corresponds to  $B$  values above that of diamond (445 GPa), that part is discarded. Figure 2 shows the 95% confidence region for the homogeneous ta-C film. The region corresponding to  $B < 445$  GPa gives values of 710-805 GPa for  $E$  and 290-385 GPa for  $G$ , the intervals for  $B$  and  $\nu$  remaining wider: 280-445 GPa and 0.03-0.23 respectively. The averages  $E = 757.5$  GPa and  $G = 337.5$  GPa give  $B = 334$  GPa and  $\nu = 0.12$ , as summarised in Table 2.

The ta-C film from single bend FCVA was not homogeneous, and was analysed by a more refined procedure. The film was modelled by two homogeneous layers: an external layer 7 nm thick with density of  $2.7 \text{ g/cm}^3$  and an internal layer 63.5 nm thick with density of  $3.24 \text{ g/cm}^3$  [11]. The MRW velocity is mainly sensitive to the (E,G) couple of the inner layer, and was used to determine it. All the data, including the MLR, were then exploited to obtain the (E,G) couple of the outer layer. Despite the homogeneous schematisation of a probable density gradient, the values  $E_{\text{int}} = 750\text{-}790$  GPa,  $G_{\text{int}} = 300\text{-}395$  GPa,  $E_{\text{ext}} = 200\text{-}300$  GPa, and  $G_{\text{ext}} = 70\text{-}150$  GPa could be determined. This shows the ability of SBS to investigate ultrathin layers.

Values obtained for the ta-C:H films from the physically plausible part of the confidence region are presented in Table 2.  $B$  remains poorly determinate, the MLR being not detectable.

## DISCUSSION AND CONCLUSIONS

We now compare our results to previous studies. Our  $E$  values are in agreement with those obtained by other SAW methods [8,13,14] which have a lower resolution than SBS but, as all SAW-based methods, are highly sensitive to Young's modulus and less sensitive to the Poisson ratio. This explains our lower accuracy for  $\nu$  and the necessity of an assumption about  $\nu$  in LISAW. On the other hand, the Oliver and Pharr analysis of nano-indentation underestimates  $E$  for ta-C, giving values of 400 -500 GPa [3,6]. Knapp et al. [15,4] proposed a finite-element model to overcome the limitations of the Oliver-Pharr analysis of the indentation curve, but their

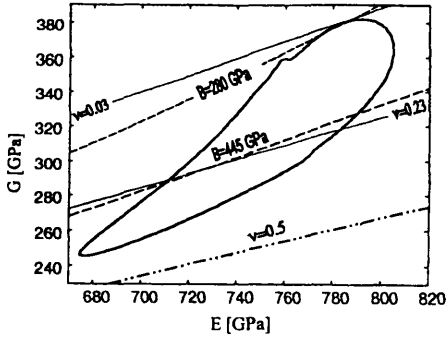


Fig. 2: The 95% confidence region (solid contour line) in the (E,G) plane for the homogeneous ta-C film:  $B=\text{const}$  (dashed) and  $\nu=\text{const}$  (dotted) lines. The region below the  $\nu=0.5$  line is a region of thermodynamic instability

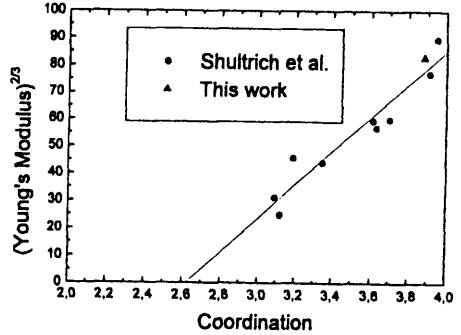


Fig. 3:  $E^{2/3}$  versus  $sp^3$  fraction for various a-C films: present result ( $\blacktriangle$ ) and data from Schultrich ( $\bullet$ ) [13].

model seems to overestimate  $E$  at 1020-1100 GPa. Our data indicate that  $E$  of ta-C:H (300 GPa, similar to values obtained by nano-indentation of thick films[5]) is much lower than that of ta-C. Clearly the hydrogen content of ta-C:H strongly reduces its network rigidity.

In Fig. 3 the modulus  $E$  of a-C films measured by SBS here or by LISAW is plotted against the  $sp^3$  fraction. The density was converted to an  $sp^3$  fraction using correlations derived from EELS and XRR [11]. The constraint-counting theory of the elastic properties of random covalent networks [1] predicts a dependence of Young's modulus on mean atomic coordination  $Z$  as

$$E = E_0 (Z - 2.4)^{1.5} \quad (2)$$

where 2.4 is the critical coordination, below which the networks have zero rigidity. Amorphous carbon networks with mixed  $sp^2$  and  $sp^3$  bonding provide a good test for this theory. The mean coordination  $Z$  depends on  $sp^3$  fraction  $x_{sp^3}$  as  $Z = 3 + x_{sp^3}$ . Fig. 3 shows that this correlation gives a reasonable fit. The intercept at  $E=0$  corresponds to a  $sp^3$  fraction of -0.4, or a coordination number of 2.6, close to the theoretical value of 2.4. Extrapolation of Fig. 3 to a coordination of 4 gives  $E \sim 800$  GPa, considerably smaller than the isotropic average modulus of diamond, 1144 GPa, and closer to the modulus found in a molecular dynamics simulation of a 100%  $sp^3$  random network of a-C [16].

This suggests that random networks may be softer than the isotropic averages of the

Table 2: Elastic constants of our films, compared to the isotropic (Voigt-Reuss-Hill) average for diamond and for the 100%  $sp^3$  random network simulation of WWW-ta-C [16]

	Ta-C:H	Ta-C	ta-C <sup>surf</sup>	WWW-ta-C	Diamond
E (GPa)	300 $\pm$ 4 <sub>-9</sub>	757.5 $\pm$ 47.5	200-300	822.9	1144.6
G (GPa)	115 $\pm$ 1 <sub>-10</sub>	337.5 $\pm$ 47.5	70-150	366	534.3
B (GPa)	248 $\pm$ 197 <sub>-0</sub>	334 $\pm$ 111 <sub>-54</sub>	>67	365	444.8
$\nu$	0.3 $\pm$ 0.09 <sub>-0</sub>	0.12 $\pm$ 0.11 <sub>-0.09</sub>	0 - 0.43	0.124	0.07

corresponding crystal. Table 2 also compares the Poisson's ratios of ta-C and ta-C:H and the isotropic average of diamond. Diamond has a uniquely low Poisson's ratio, and the value of ta-C is similar, presumably due to the same high bond angle rigidity of carbon's sp<sup>3</sup> bonds. The higher value (0.3 - 0.4) of Poisson's ratio of a-C:H indicated by Jiang et al. [2] is consistent with our result for ta-C:H:  $\nu \sim 0.3$ . This suggests the C-H bonding in both ta-C:H and a-C:H tends to increase Poisson's ratio.

In conclusion, we have shown that surface Brillouin scattering is the best technique to measure the elastic constants of thin and, particularly, very thin supported films. An appropriate data analysis of the modified Rayleigh wave dispersion relation allows a precise estimate of Young's modulus and shear modulus also in the case of fast films on slow substrates, typical of hard DLC films. When a second branch, namely the high frequency pseudo surface wave, is measurable, the bulk modulus becomes directly accessible.

## ACKNOWLEDGEMENTS

M.G.B., C.E.B. and R.P. acknowledge financial support from "Progetto Finalizzato Materiali Speciali per Tecnologie Avanzate II" of Consiglio Nazionale delle Ricerche. A.C.F. acknowledges funding by an E.U. TMR fellowship.

## REFERENCES

- [1] H. He, M F Thorpe, *Phys. Rev. Lett.* **54** 2107 (1985)
- [2] X. Jiang, K. Reichelt and B. Stritzker, *J. Appl. Phys.*, **68**, 1018 (1990)
- [3] G.M. Pharr, D.L. Callahan, S.D. McAdams, T.Y. Tsui, S. Anders, J.W. Ager, I.G. Brown, C.S. Bhatia, S.R.P. Silva and J. Robertson, *Appl. Phys. Lett.*, **68**, 779 (1996)
- [4] T.A. Friedman, J.P. Sullivan, J.A. Knapp, D.R. Tallant, D.M. Follstaedt, D.L. Medlin and P.B. Mirkarimi, *Appl. Phys. Lett.*, **71**, 3820 (1997)
- [5] M. Weiler, S. Sattel, T. Giessen, K. Jung, H. Ehrhardt and J. Robertson, *Phys. Rev. B*, **53**, 1594 (1996)
- [6] S. Xu, D. Flynn, B.K. Tay, S. Praver, K.W. Nugent, S.R.P. Silva Y. Lifshitz and W.I. Milne, *Phil. Mag. B*, **76**, 351 (1997)
- [7] M.G. Beghi, C.E. Bottani, P.M. Ossi, T. Lafford and B.K. Tanner, *J. Appl. Phys.*, **81**, 672 (1997), and references therein
- [8] D. Schneider, C.F. Meyer, H. Mai, B. Schoeneich, H. Ziegele, H.J. Scheibe and Y. Lifshitz, *Diam. and Rel. Mat.*, **7**, 973 (1998)
- [9] P. J. Fallon, V. S. Veerasamy, C. A. Davis, J. Robertson, G. A. J. Amaratunga, W. I. Milne, *Phys. Rev. B*, **48**, 4777 (1993); M. C. Polo, J. L. Andujar, J. Robertson and W. I. Milne, *Diamond. Relat. Mater.*, to be published (1999).
- [10] M. Weiler, K. Lang, E. Li, J. Robertson, *Appl. Phys. Lett.*, **72**, 1314 (1998); N.A. Morrison, S.E. Rodil, A.C. Ferrari, J. Robertson and W. I. Milne, *Thin Solid Films*, **337**, 71 (1999)
- [11] A. Libassi, A.C. Ferrari, V. Stolojan, B.K. Tanner, J. Robertson, L. M. Brown, *Diamond and Related Materials*, to be published (1999)
- [12] A.C. Ferrari, J. Robertson, M.G. Beghi, C.E. Bottani, R. Ferulano and R. Pastorelli, *Appl. Phys. Lett.* **75**, 1893 (1999)
- [13] B. Schultrich, H. J. Scheibe, D. Drescher and H. Ziegle, *Surf. Coat. Tech.* **98**, 1097 (1998)
- [14] C. J. Morath, H. J. Maris, J. J. Cuomo, D. L. Pappas, A. Grill, V. V. Patel, J. P. Doyle and K. L. Saenger, *J. Appl. Phys.* **76**, 2636 (1994)
- [15] J.A. Knapp, D. M. Follstaedt, S. M. Myers, J. C. Barbour and T. A. Friedmann, *J. Appl. Phys.* **85**, 1460 (1999)
- [16] P. C. Kelires, *Phys. Rev. Lett.* **73**, 2460 (1994)